Universitat de les Illes Balears

Facultat de ciències

Curva de respuesta de fase de un circuito neuronal
Phase response curve of a neuronal circuit

Beatriz Mato Mora

Grau de física

Any acadèmic 2014-15

DNI de l'alumne: 43195471E

Treball tutelat per Claudio Mirasso Santos
Departamento de física

Paraules clau del treball:
Sistemas complejos, Biofísica, Neurociencia, Curva de respuesta de fase, Sincronización

Contents

Everything we do, every thought we've ever had, is produced by the human brain. But exactly how it operates remains one of the biggest unsolved mysteries, and it seems the more we probe its secrets, the more surprises we find. - Neil deGrasse Tyson.

1.   Introduction

With around 10^{11} neurons in the nervous system transmitting information amongst them, the study of these cells is of crucial importance to gain an understanding of the brain, which is considered by many to be one of the most complex systems in nature. Each neuron has about 10000 connections with others, through which they transmit electrical pulses, passing on information, thus controlling the behaviour of our system.

To have a good understanding of neurons, it is interesting to investigate how they connect, firstly in neuronal circuits formed of few neurons, which is the main focus of this work. Neurons then establish networks, the study of which should lead up to gain an insight into the workings of brain as a whole, and, finally, of our system. On the other hand, studies can go from the neuronal level down to cell biophysics and molecular biology as well [1].

Neurons achieve information transmission through electrical pulses. These pulses are a response to chemical or electrical inputs from other neurons, called synapses, which cause ion concentrarion within the neuron to vary with respect to the extracellular medium due to the opening of ion channels. This variation generates a spike in the membrane potential of the cell, which is then transmitted along the neuron, and afterwards to other neurons. The electrical pulses represent different information according to the various temporal patterns in which they fire. Synapses may be either chemical or electrical:

- *Chemical:* the electrical activity in the presynaptic neuron activates the release of neurotransimitters, chemical substances that are released into the synaptic cleft, and are then received by postsynaptic neuron. The neurotransmitters bind to receptors in the postsynaptic neuron, which induce the ion channels to open. Depending on the type of the neurotransmitter that is released, the postsynaptic neuron will suffer a depolarization or hyperpolarization of the membrane potential, respectively exciting or inhibiting the cell membrane. The principal excitatory neurotransmitter is glutamate, with two different types of receptors: AMPA are responsible for rapid transference of currents, whereas NMDA activates and deactivates the postsynaptic membrane channels more slowly. For inhibitory synapses, the main neurotransmitter is GABA, which also has two types of receptors: $GABA_A$ for fast transmission and $GABA_B$ for slow. [2].

- *Electrical:* neurons are directly connected through gap junctions, special channels which allow electrical currents to move directly between neurons.

Throughout this work, chemical synapses will be used.

As explained, synapses produce a membrane potential in the postynaptic neuron. The neuron will generate a spike - or not. Neurons may be classified in accordance to the mechanisms through which an action potential is created:

- *Integrators:* as Izhikevich states in [1], these neurons sum postsynaptic potentials and compare them to a threshold voltage value; if the sum is below the threshold, then the neuron is at rest, and it fires a spike when the membrane potential is above the threshold, returning to rest afterwards.

- *Resonators:* in contrast, these neurons do not fire an all-or-none spike, but rather, they show subthreshold oscillations [1].

In 1952, Hodgkin and Huxley studied the ionic currents across the membrane of the squid giant axon, and the propagation of action potentials in it, introducing a set of variables that characterize the state of the system, and a set of equations that describe the temporal evolution of said variables [3]. This description is that of a dynamical system, so it can be concluded that neurons are in fact dynamical systems. When treating neurons as dynamical systems, the state variables can be classified, as Izhikevich writes [1], into four classes:

I Membrane potential.

II Excitation variables, which facilitate the generation of a spike.

III Recovery variables. Once the neuron has spiked, these variables help it go back to rest.

IV Adaptation variables, which influence spiking in the long term.

The first model that introduced dynamical equations for the state variables of the neuron was that of Hodgkin and Huxley (1952) [3]. In a series of papers, they studied the membrane of the squid giant axon, and concluded that it could be represented by an electrical circuit, that can be seen in Figure 1a, where the membrane was characterized as a capacitor, and the ionic channels were represented by a resistor and a voltage source, which represents the equilibrium potential for each channel. All these elements were set in a parallel configuration, thus describing the voltage difference between the interior of the membrane and the exterior. They then go onto proposing a model which would describe the membrane potential, V, and the ionic channels activation and inactivation rates. The activation rate for the sodium ionic channels is m, whereas h is the inactivation rate for Na^+ channels. Potassium ionic channels are modelled by activation rate n. The ion channels are illustrated in Figure 1b, where the activation and inactivation gates can be seen. Hodgkin and Huxley analysed the ionic conductances in the squid giant axon, and attained a system of equations for the model known as the Hodgking-Huxley model.
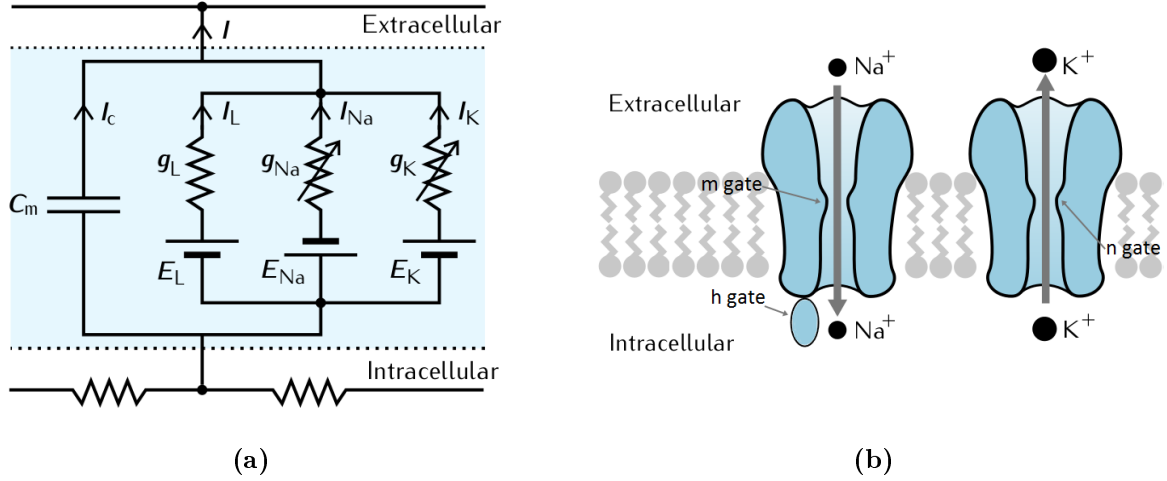
Figure 1: (a) Hodgkin and Huxley described the membrane as an electrical circuit. **(b)** Ion channels. Both figures adapted from Sterratt et al. [4]

The system of equations proposed by Hodgkin and Huxley is [3]:

$$C_m\frac{dV}{dt} = \bar{g}_K n^4(E_K - V) + \bar{g}_{Na}m^3 h(E_{Na} - V) \tag{1a}$$

$$+\bar{g}_m(E_{rest} - V) + I + \sum I_{syn}$$

$$\frac{dn}{dt} = \alpha_n(V)(1 - n) - \beta_n(V)n \tag{1b}$$

$$\frac{dm}{dt} = \alpha_m(V)(1 - m) - \beta_m(V)m \tag{1c}$$

$$\frac{dh}{dt} = \alpha_h(V)(1 - n) - \beta_h(V)h \tag{1d}$$

where C_m is the membrane potential, E_K, E_{Na} and E_{rest} represent the equilibrium potentials for potassium, sodium and leakage currents, respecively, I is a constant current and $\sum I_{syn}$ is the sum of the synaptic currents received by the neuron. The activation and inactivation rates depend upon the experimetally fitted expressions [3]:

$$\alpha_n(V) = 0{,}01\frac{10 - V}{e^{10-V/10} - 1} \tag{2a}$$

$$\beta_n(V) = 0{,}125e^{-V/80} \tag{2b}$$

$$\alpha_m(V) = 0{,}1\frac{25 - V}{e^{25-V/10} - 1} \tag{2c}$$

$$\beta_m(V) = 4e^{-V/18} \tag{2d}$$

$$\alpha_h(V) = 0{,}07e^{-V/20} \tag{2e}$$

$$\beta_h(V) = \frac{1}{e^{30-V/10} + 1} \tag{2f}$$

This is a four-dimensional dynamical model.

Subsequent studies introduced new conductance-based models. A few of these models are: the Morris-Lecar model [5] is a two-dimensional model which describes the action potential of the membrane with an activation rate for potassium channels, and a rapid rate for calcium channels; the integrate and fire model [6] is a one-dimensional model, in which the membrane potential increases until it reaches the threshold, when the neuron fires a spike and is then reset; or the Izhikevich model [7], that reduces the four-dimensional model of Hodgkin and Huxley to a two-dimensional one, with a resetting of the membrane potential after it spikes. Each model may describe a different type of neuron in terms of their firing patterns. These are some among many others of the firing patterns into which neurons may be classified [6]: tonic spiking, when it can be induced to fire a train of spikes; phasic spiking, when there is only one spike; tonic bursting, when it fires bursts of spikes with a given perioidicity; or phasic bursting, when the neuron fires a single burst of spikes. These, as well as some other firing patterns, are illustrated in Figure 2.

Since these dynamical systems of equations generally do not have an analytical solution, one must evaluate the implementation cost as well as the biological plausibility of the model. In his work [6], Izhikevich explains that the neuronal model which should be used depends upon the problem that is trying to be solved. For example, the Hodgkin-Huxley model is biologically plausible, but very expensive to implement, whereas the integrate and fire model is very efficient, but lacks biological plausibility. It is important to know that not all models can exhibit the same firing patterns, therefore one must have a deep understanding of the problem trying to solve, in order to wisely choose the most appropiate model.

In this work, the connections between two and three neurons will be analysed. Because the number of neurons that will be represented is low, the Hodgkin-Huxley model can and will be used, as it is more biologically plausible than other models, and it is able to be implemented without problems.
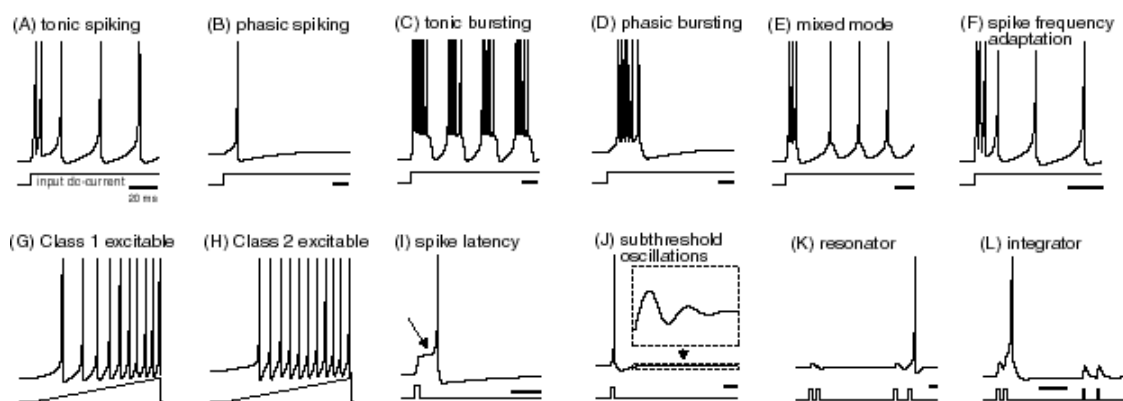

Figure 2: Examples of neuronal firing patterns. Electronic version of the figure and reproduction permissions are freely available at *www.izhikevich.com*

As well as classifiable in accordance to spike generation or temporal patterns, neurons can be classified by the response the membrane has to inputs. Neurons have three types of excitabilities [8]:

I Type I excitability: the membrane can be induced to oscillate at an arbitrarily low frequency.

II Type II excitability: there can only be oscillations above a non-zero frequency.

III Type III excitability: the neuron does not exhibit oscillations unless perturbed at high frequencies, and even so may fail to show repeated oscillations, and only exhibit one.

As neurons are dynamical systems, it can be of interest to represent one dynamical variable against another in a phase portrait, in order to see their trajectories and study the dynamics of the system. Within this representation, one can find limit cycles, which are closed trajectories in the phase space [1]. Limit cycles represent periodic solutions to the dynamical system, that is, they are descriptions for self-sustained oscillators in the phase space, and these cycles are stable to small perturbations. When the limit cycle is perturbed, the oscillator will return to its original state, although it will do so with a phase change [11]. An example of a limit cycle for the Morris-Lecar model can be seen in Figure 3, shown in red; the black lines represent small perturbations that return to the limit cycle.
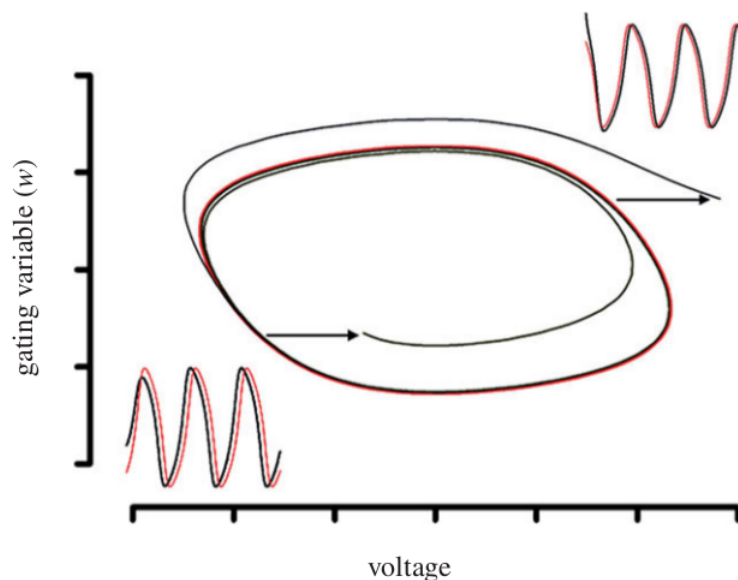

Figure 3: A stable limit cycle for the Morris-Lecar model. Perturbations on the limit cycle return rapidly to it. This is also seen in the voltage time series shown in the two corners. Figure extracted from Smeal et al. [11].

2.   Phase response curve

Neurons, when described as dynamical systems in the conductance based models explained earlier in this work, present self-sustained oscillatory patterns. Hence, when a neuron receives a synaptic input, the original oscillation of said neuron is perturbed. In this section, the synchronization of two different neuronal circuit configurations will be studied. In particular, the changes in the oscillation of the postsynaptic neuron will be analysed.

When neurons interact with each other, their self-sustained periodic oscillations can adjust due to the interaction, that is, they can reach a synchronized state [9]. As Smeal et al. summarise in [11], various studies have shown that synchronization in the brain is important for a normal physiological functions, but also leads to neural diseases, such as Parkinson's disease, schizophrenia, autism or epilepsy. Achieving a better understanding of neuron sychnronization, and what factors contribute to it, might lead to controlling it.

One of the most important tools to analyse the response of an oscillator when it is subject to a perturbation is the phase response curve (PRC). A PRC is useful to measure the effect that a precisely timed perturbation has on the cycle of an oscillator [10]. The timing of the perturbation will have a huge impact on the variation of the cycle period. This can be seen in Figure 4. In this example, Smeal et al. apply a perturbation to the oscillator depicted in Figure 4a, and they do so at different times in the cycle, as indicated by the arrows. In this example, it can be seen in Figures 4b, 4c and 4d that the period is shortened. Some other examples show, however, that the period of the oscillator can also be lengthened. Therefore, the period T of a free running periodically spiking neuron varies when the limit cycle is perturbed. The phase response curve represents this change, measured as a function of the time of the perturbation t. Although PRC represents the shifts in the phase of oscillation, these can be converted to time delays or advances. The timing at which the oscillator is applied is measured relative to an event that occurs at the same time in the cycle of the free running neuron [11]; this point is arbirtrary, and in this work the timing is measured with respect to the peak of the membrane potential.
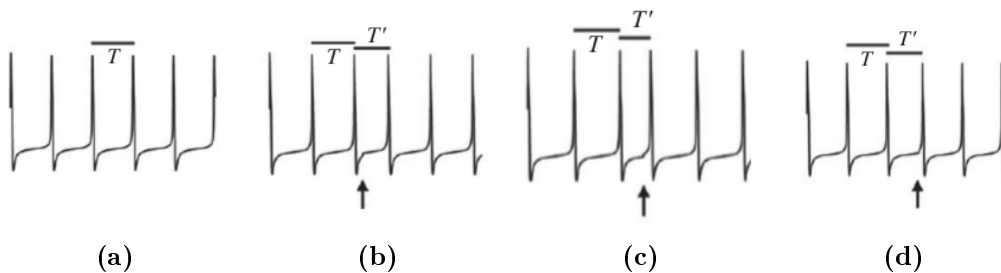

(a)   (b)   (c)   (d)

Figure 4: Example of the change of a limit cycle when it is perturbed. Figure extracted from Smeal et al. [11].

The PRC is defined as follows [9]:

$$PRC(t) = t_{spike}^{free} - t_{spike}^{disturbed} \qquad (3)$$

where t_{spike}^{free} is the time when the free neuron spikes, and $t_{spike}^{disturbed}$ is the time when the disturbed neuron does so. If the disturbed neuron fires after it would if it were running free, then the $PRC(t) < 0$, and so, the next spike is delayed. On the contrary, if $PRC(t) > 0$, then the next spike is advanced, which means that the disturbed neuron fires before it would without a perturbation. Some neurons will show time delays and advances in their PRCs, whereas some others only show advances. This allows the following classification for phase response curves [10]:

I Type I, the phase only shows advances when the postsynaptic neuron is depolarized.

II Type II, the phase can either be advanced of delayed, depending on the timing of the perturbation.

In Figure 5, the definition and types of PRCs are illustrated.

The shape of the PRC depends upon the shape of the stimulus, as well as on the dynamics of the oscillator being perturbed. Ermentrout shows in his work [12] that the types of PRC can be related to the different classes of excitable membranes. This is the case because of the mechanism by which the neuron spikes periodically. Type I excitable membranes are associated with type I PRC, whereas neurons with type II excitability show type II PRCs.

One of the biggest advantages of studying phase response curves is that it can be assessed experimentally, which means that the theoretical predictions can be tested. The dynamics of the neuronal components of the network are theoretically linked to
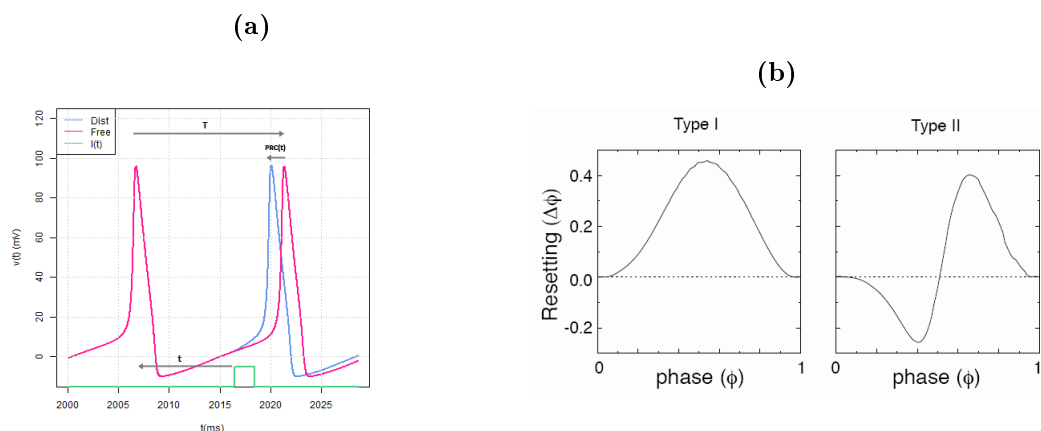

Figure 5: Phase response curve definition and properties. **(a)** Definition of the PRC. **(b)** Neurons can exhibit two types of phase response curves. Figure extracted from Canavier [10].

the characteristics of the network's synchronization through the phase response curve, so, via the PRC, the dynamics of the network can be related to neuron biophysics in a manner that can be experimentally measurable. Smeal et al., in their review over PRCs and synchronized networks [11] give an example of the experimental assessability of the phase response curve. They explain the theoretical work carried out by Best and later experimentaly verified by Guttman et al., in which the PRC theory predicted that when the squid giant action was periodically oscillating, a small perturbation in the form of a current injection could extinguish the ongoing spiking oscillations.

2.1.   Neuron motifs

In this work, the synchronization between two and three neurons were analysed, through the numerical calculation of their PRCs. They were studied in two motifs: master-slave, where two neurons are unidirectionally coupled, and master-slave-interneuron, where a third neuron is added, acting as an inhibitory loop, found to play a role in the anticipated response of some neuronal circuits in the brain [9]. These are further explained later.

The model chosen for the study of these networks is the Hodgkin-Huxley model, which was presented in the introduction. This model consists of four differential equations as written in the set of equations (1), which describe the membrane potential and the gating variables for the ionic channels. This model presents a type II phase response curve, since it has a type II excitable membrane.

2.1.1.   Neuron model and synaptic coupling

The model that Hodgkin and Huxley proposed is characterized by equations (1a), (1b), (1c) and (1d). In these equations, the membrane is described as an electrical circuit, in which the membrane is characterized as a capacitor, and the ion channels as resistors in series with a voltage source, which represents the equilibrium potential of each channel; an implemented current I is also shown in the equations. For the numerical calculations carried out here, the parameters for the set of equations (1) can be found in Table 1 [9].

$\mathbf{C_m\,(\mu F)}$	9π	$\mathbf{\bar{g}_{Na}\,(mS)}$	1080π
$\mathbf{I\,(pA)}$	280	$\mathbf{E_{Na}\,(mV)}$	115
$\mathbf{\bar{g}_K\,(mS)}$	324π	$\mathbf{\bar{g}_m\,(mS)}$	$2{,}7\pi$
$\mathbf{E_K\,(mV)}$	-12	$\mathbf{E_{rest}\,(mV)}$	10.6

Table 1: Parameters employed in the Hodgkin-Huxley model for numerical calculations.

In the model, the neurons are coupled through chemical synapses, and it can be excitatory or inhibitory. Depending on whether the synapse is excitatory or inhibitory, the type of receptors in the postsynaptic neuron will be AMPA and GABA respectively. The fraction of synaptic receptors, r^i ($i = A, G$) for AMPA and GABA, in the postsynaptic neuron is described by the equation [9]:

$$\frac{dr^i}{dt} = [T]\alpha_i(1 - r^i) - \beta_i r^i \tag{4}$$

where α_i and β_i are rate constants and $[T]$ is the concentration of neurotransmitters in the synaptic cleft, which is a function of the presynaptic potential:

$$[T](V_{pre}) = \frac{T_{max}}{1 + e^{-(V_{pre}-V_p)/K_p}} \tag{5}$$

where $T_{max} = 1\,mM^{-1}$ is the maximum value of neurotransmitter concentration, $K_p = 5\,mV$ gives the steepness of the sigmoid and $V_p = 62\,mV$ sets the value at which the function is half-activated. The concentration of neurotransmitters is not time dependent, from which it is assumed to be an instantaneous function.

The synaptic current is given by:

$$I^i = g_i r^i(E_i - V) \tag{6}$$

where V is the postsynaptic potential, g_i is the maximal conductance and E_i the reversal potential. It should be noticed that the synaptic current is a function of both the postsynaptic current, directly in the definition, and the presynaptic current, through the fraction of bound neurotranmitters in the synaptic cleft. The synaptic current, thus, couples both master and slave neurons together.

Throughout the numerical calculations carried out here, the synaptic coupling parameters that were used are detailed in Table 2 [9], unless stated otherwise, as will be done in the case of the master-slave motif. In that scenario, the maximal conductance for the excitatory synapse will be varied to analyse the effect this has on the phase response curve.

$\boldsymbol{\alpha_A}$ (mM⁻¹ms⁻¹)	1,1	$\mathbf{E_A}$ (mV)	60
$\boldsymbol{\beta_A}$ (ms⁻¹)	0,19	$\mathbf{E_G}$ (mV)	−20
$\boldsymbol{\alpha_G}$ (mM⁻¹ms⁻¹)	5,0	$\mathbf{g_A}$ (nS)	1
$\boldsymbol{\beta_G}$ (ms⁻¹)	0,30	$\mathbf{g_G}$ (nS)	2

Table 2: Parameters used for the synaptic coupling

(a) Master-Slave configuration.   **(b)** Master-Slave-Interneuron configuration.
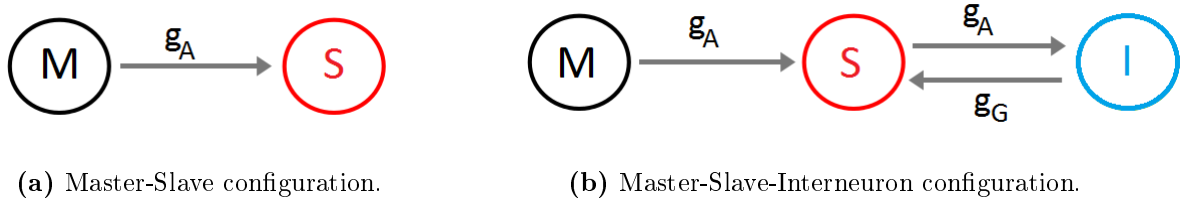
Figure 6: Two neuronal motifs employed in this work.

2.1.2.   Two and three neuron motifs

For the purposes of the present work, two neuronal motifs will be studied:

I **Master-slave:** in this configuration, two neurons are coupled unidirectionally. The neuron motif can be seen in Figure 6a; here, the slave neuron is perturbed by the master, which remains unperturbed.

II **Master-slave-interneuron:** in this scheme, a third neuron is added to the previous motif, which is shown in Figure 6b. Just like before, the master is unidirectionally coupled to the slave, which is in turn coupled to an interneuron, now in a bidirectional configuration. The slave receives an inhibitory input from the inteneuron, and the latter is perturbed by an excitatory synapse from the slave.

2.1.3.   Master-Slave

In this work, the synchronization of the neurons is analysed throught the PRCs, in order to predict the behaviour for square current (theoretical) inputs, and biologically plausible synapses.

For this motif, different numerical calculations were carried out. Firstly, the synapse between the master neuron and the slave was substituted by a rectangular function of height H and length L. A type II phase response curve is expected, since the Hodgkin-Huxley model has a type II excitability [11]. Rectangular current pulses of different heights and lengths were used to perturb the limit cycle, and their PRCs obtained. Since this cannot happen naturally in two coupled neurons, these results are a theoretical prediction to study the behaviour of the slave neuron when pertubed. This calculation was previously carried out by Matias in her thesis [9], and the PRCs compare exactly to her work. Secondly, the phase response curve of a master-slave configuration was found for a biologially plausible synapse, as described in Section 2.1.1. The PRC was generated for excitatory synapses and three different maximal synaptic current conductances. In order to obtain the PRC, the perturbations are applied at different times of the limit cycle in all cases.
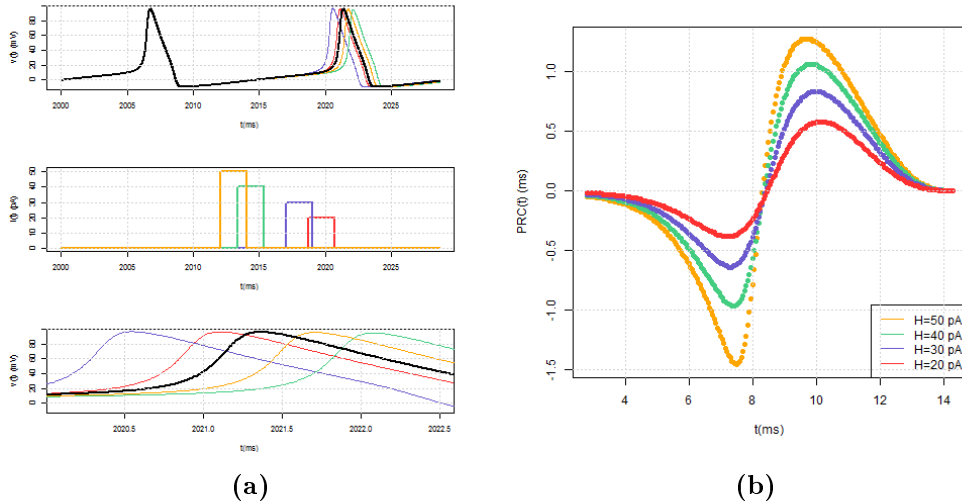
Figure 7: (a) Rectangular pulses of different heights perturb the slave neuron at various times. Top figure shows the membrane potential for the intensities applied in the middle figure at those particular times, in a colour coordinated manner. The black line in the top figure represents free running neuron. Bottom figure zooms into the peak of membrane potential after the current is applied. **(b)** PRC for fixed $L = 2\,ms$ and varying height.

Rectangular current inputs with same length and different heights

The first case studied was the phase response curve when rectangular input currents with the same length, $L = 2\,ms$, but different heights were applied to the limit cycle. In Figure 7a, examples of the various currents with specific heights are illustrated: in the middle figure, the different height input currents are shown perturbing the neuron at a particular time, which results in the membrane potential of the slave neuron being either advanced or delayed, depending on the timing of the perturbation. The phase shifts are portrayed in the top figure of 7a, that shows the membrane potential of the ditrubed neurons, seen in colour, with respect to the black free running neuron. This delay or advance can be more closely seen in the bottom figure, as it shows a zoom of the peak of action potential.

The phase response curve was computed for the various currents of same length and distinct heights, the result of which is illustrated in Figure 7b. It is evident from this figure that the higher the amplitude of the current for the same length, the more delayed or advanced the distrubed neuron will be with respect to the free running neuron. It is also noteworthy that the disturbed neuron changes the synchronization regime for the same perturbation time, progressing from delayed to advanced at precisely the same time.

As was expected, the phase response curve is a type II PRC, since the model used for the numerical implementation was the Hodgkin-Huxley model, which has type II excitability.
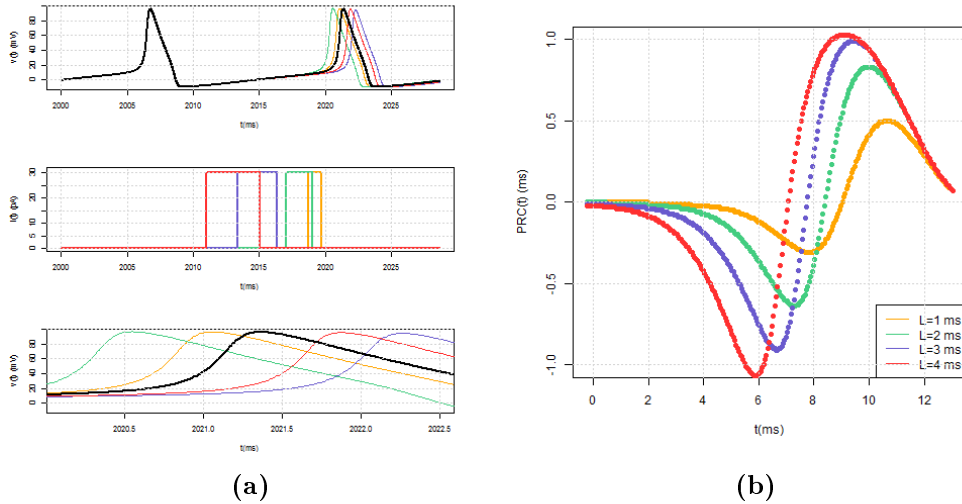
Figure 8: (a) Rectangular pulses of different lengths perturb the slave neuron at various times. Top figure shows the membrane potential for the intensities applied in the middle figure at those particular times, in a colour coordinated manner. Black line in the top figure represents free running neuron. Bottom figure zooms into the peak of membrane potential after the current is applied. **(b)** PRC for fixed $H = 30\,pA$ and varying length.

Rectangular current inputs with same height and different lengths

As with the rectangular current with different height for the same length, the phase response curve was determined for a current of specific height, $H = 30\,pA$, and different lengths. In Figure 8a, the different current inputs are illustrated. In an equivalent manner, the middle figure represents the intensities of various heights, perturbing the slave neuron at distinctive times, the membrane potential of which is depicted in the top figure, being delayed or advanced as the intensity disturbs the limit cycle. Shown in black is the free running neuron. Like before, the bottom image portrays the peak of membrane potential for the disturbed neurons.

Represented in Figure 8b is the phase response curve calculated for the currents of varying durations. Analogously to the different heights for the same length, the longer the pulse the bigger the delay or advance in the disturbed neuron. However, in this scenario, some dissimilarities appear with respect to the aforementioned situation. In contrast with the previous case, the system changes dynamics at a different time for each of the lengths used to compute the PRC, which is also seen as the curve starts its delay as the perturbation is further apart from the previous spike for the shorter pulses. Even though it is noticeable that the longer current has a bigger phase response curve, the shape remains the same for all lengths.

Just like before, the phase response curve can be identified as a type II PRC.
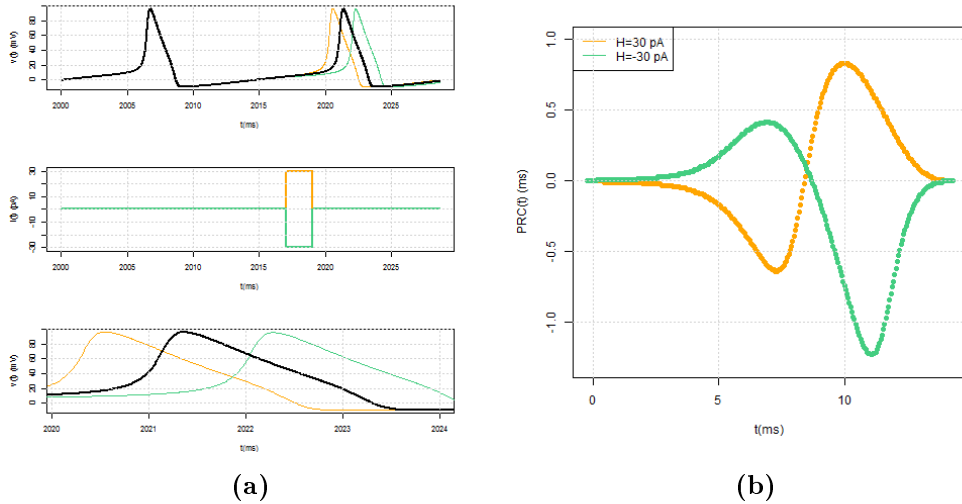
Figure 9: (a) Rectangular pulses equivalent to excitatory and inhibitory synapses. Top figure shows the membrane potential for the intensities applied in the middle figure at those particular times. Bottom figure zooms into the peak of membrane potential after the current is applied. **(b)** PRC for excitatory and inhibitory equivalent synapses.

Rectangular current inputs for positive and negative pulses

In this study, the excitatory and inhibotry synapses are substituted by a positive and negative rectangular current, respectively. These pulses are of the same height and length, with the exception of the sign. The length of the pulse is $L = 2\,ms$, and its height is $H = \pm 30\,pA$.

Shown in the top of Figure 10a are the membrane potentials of the neurons: seen in colour are the disturbed neurons, and in black is the free neuron. To illustrate the differences between the excitatory and inhibitory cases, in the example in the middle figure the plotted times of the perturbations are the same, to show that if the excitatory input advances the spike, the inhibitory will delay it. From this representation it could be predicted that the phase response curve for the inhibitory synapse would be of opposite sign. The bottom figure of Figure 10a amplifies the area of the peak membrane potential.

As was done in the previous scenarios, the phase response curve was calculated. The result for the PRC is represented in Figure 10b. It can be seen that, as expected, the phase response curve is of opposite sign for the inhibitory pulse as the excitatory. However, it is very clear that the inhibitory current is not a mere reflection of the excitatory one, as the maximum values of the curves are not identical. It is also noticeable that the shape of the PRC is similar, but not an exact opposite. The inhibitory pulse creates a bigger delay than the excitatory one, and this disparity in phase shifts is also obvious in the advanced spikes, as the excitatory current advances the spikes to a greater difference with respect to the free running neuron.
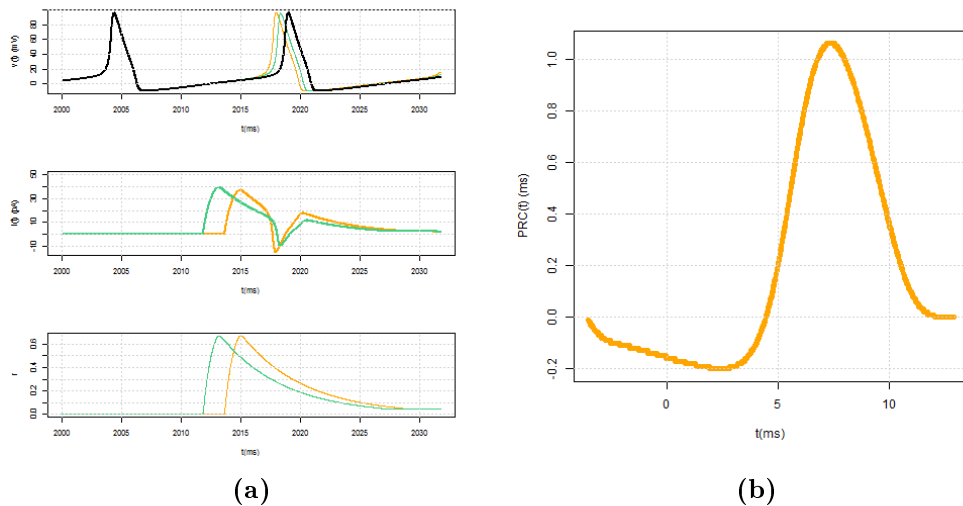
<div align="center">(a)   (b)</div>

Figure 10: (a) Biologically plausible synaptic current, for $g_A = 1\,nS$. Illustrated in the top picture, the membrane potential for a free running neuron is shown in black; coloured lines show the membrane potential for disturbed neurons, perturbed by synaptic currents represented in the middle figure, determined using equation (6). Bottom picture represents the fraction of bound neurotransmitters. **(b)** Phase response curve for biologically plausible excitatory synapse.

Biologically plausible synaptic current inputs

After the study of the phase response curve for simple theoretical rectangular pulses, a more biologically plausible synapses is computed, using equations (4) through to (6). For this section, only an excitatory synapse was used. The synaptic current is defined by equation (6), and here three different maximal synaptic conductances will be employed.

To begin with, an excitatory synaptic current with the parameters introduced in Table 2 is used to perturb a slave neuron at different times. An example of this is portrayed in Figure 10a. Synaptic current is represented in the middle figure, which shows two different currents for different times. It is obvious from this image that the currents do not remain the same, as they are a funciton of the postynaptic current (top of figure), as well as the fraction of bound neurotransmitters (shown at the bottom of the figure), which causes it to vary for each instance.

Calculating the time differences between spikes as a function of the time at which the neuron is disturbed, the phase response curve was obtained for the synaptic current. This result can be seen in Figure 10b. Having used an excitatory synapse for a Hodgkin-Huxley model, a type II phase response curve is attained, which presents delays for perturbations that are close to the peak of the previous, undisturbed membrane potential, and shows advances for currents that are further apart from said peak. This result can be compared to that obtained using rectangular currents. In both cases, for excitatory synapses the behaviour of the perturbed spike is the same, as it is delayed for perturbations near the
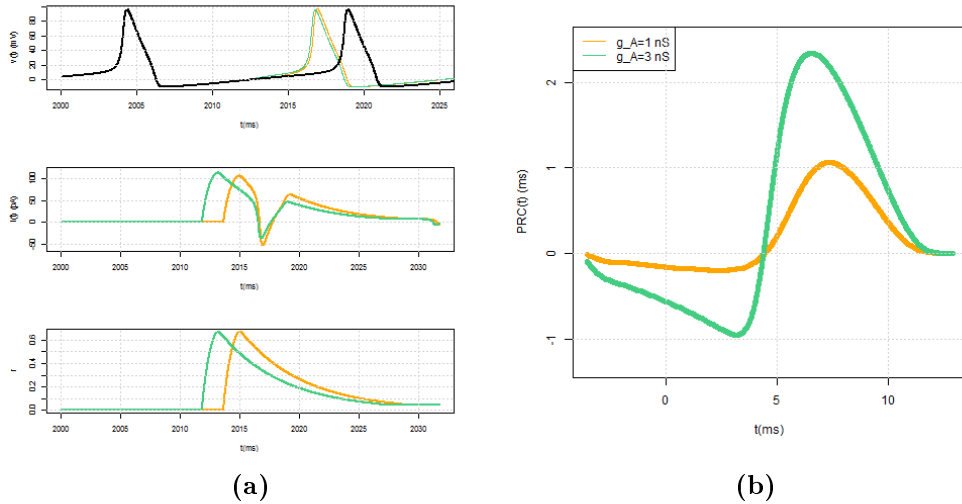
Figure 11: (a) Biologically plausible synaptic current, for $g_A = 3\,nS$. Illustrated in the top picture, the membrane potential for a free running neuron is shown in black; coloured lines show the membrane potential for disturbed neurons, perturbed by synaptic currents represented in the middle figure, determined using equation (6). Bottom picture represents the fraction of bound neurotransmitters. **(b)** Phase response curve for biologically plausible excitatory synapse.

previous spike, and advanced for the latter ones. They are also alike in the sense that the delays of the perturbed neuron with respect to the free running one are less in magnitude than the advances. However, for the rectangular currents, the neuron gets more delayed than for the synaptic current. Since the synaptic current depends on the voltage, it does not remain the same for each instance, leading to the disparity between PRCs. However, even though the results are not exact, the overall behaviour for the phase response cuvre of the biologically plausible current is comparable to that obtained in the more theoretical rectangular pulse.

The previous analysis was carried out for an excitatory synapse with a maximal conductance $g_A = 1\,nS$ for the synaptic current. Subsequently, it is interesting to analyse the effect of a varying maximal conductance for the current. Used in this case is a conductance of $g_A = 3\,nS$; the rest of the parameters needed to obtain the synaptic current are those in Table 2. In Figure 11a, the top figure represents the membrane potential for the free running neuron, shown in black, and the potentials for the disturbed neurons, which are perturbed by the synaptic currents portrayed in the middle figure. Like in the previous case, the bottom figure shows the fraction of bound neurotransmitters. In the middle figure it is also obvious that the synaptic current behaves differently at different times, due to its dependance on the postsynaptic potential.

For this case, the phase response curve is represented in green Figure 11b, along with the previously obtained PRC for the synaptic current corresponding to maximal conductance $g_A = 1\,nS$ seen in orange. In both cases, the phase response curve shows a
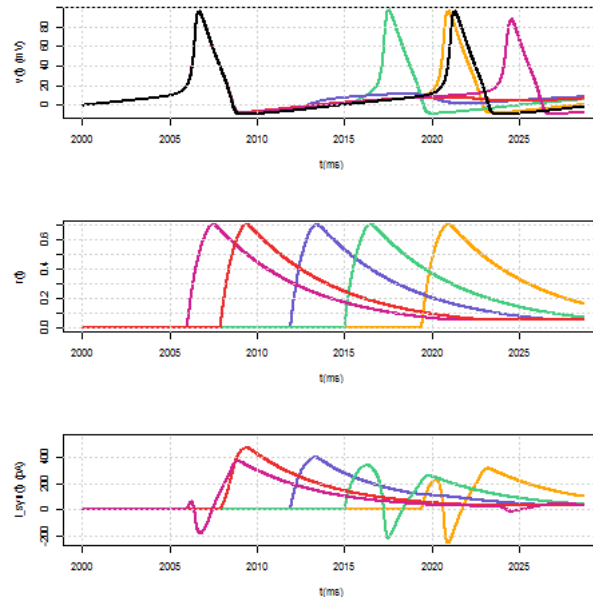
Figure 12: Death by delay. The perturbed neuron stops spiking for a range of timing of perturbation of the neuronal limit cycle, as seen for the cases of the blue and red currents in the bottom picture, with neurotransmitter fraction of the same colours in the middle figure, which do not result in a membrane spike, as observed in the top of the figure.

type II behaviour, and the aforementioned properties are mantained. As it was expected, the PRC for the current with a greater conductance has bigger delays and advances. This compares well to the previously obtained results for the rectangular currents. The change in synchornization regime occurs at the same time, equivalently to what was achieved in the case for rectangular currents of the same lenght and different heights. Thus, the theoretical results for the rectangular pulses compare to those obtained for a biologically plausible synapes, even as the shape of the phase response curve varies, as it preserves the properties.

To finalize the studies for the master-slave motif, a third maximal conductance is used, yielding results that were not initially expected. For this case, the synaptic current was computed for a maximal conductance of $g_A = 10\,nS$. As has been done for all previous scenarios, the neuron was perturbed with the synaptic current at different times of its limit cycle. In the present context, however, the membrane potential did not respond in the same way as before. This result can be seen in Figure 12. In the middle image, the neurotransmitter fraction is depicted, and it can be seen that this remains constant throughout the cycle. The synaptic current, represented in the bottom figure, does not have the same behaviour. As occured throughout the master-slave analysis, the current changes due to its dependance on the postsynaptic voltage. However, in contrast to the two previous cases, for a range of timing of perturbation, the neuron does not exhibit a spike in its membrane potential, as seen in the top of Figure 12. For the red and blue
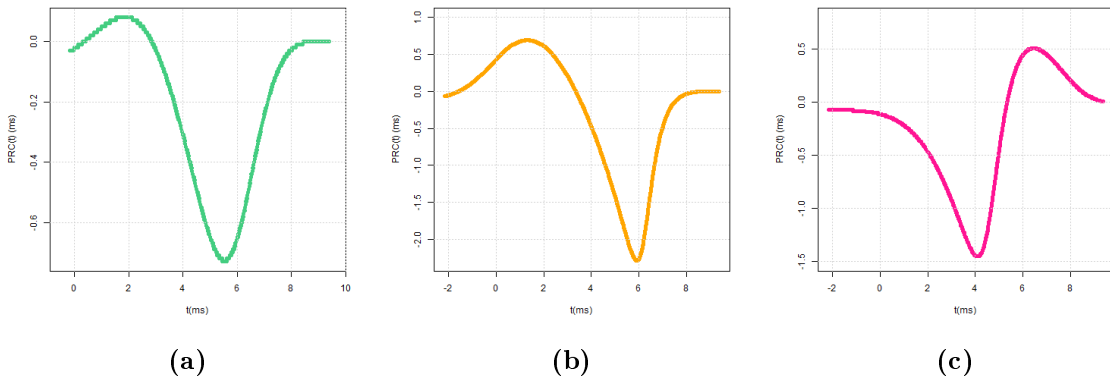
Figure 13: Phase response curves for the MSI motif with biologically plausible synaptic current. **(a)** Excitatory and inhibitory synapse perturbing the neuron at the same time. **(b)** Inhibitory current arrives at the neuron before the excitatory does. **(c)** Excitatory synapse disturbs the slave neuron before the inhibitory.

intensities, the voltage potential fails to spike, showing only subthreshold oscillations. For the earlier perturbation seen in pink, this is not the case, as it fires a delayed spike. For later perturbations, the membrane potential shows spikes again. For a range in the middle, however, the neuron does not spike.

Strogatz summarises in [13] the work carried out by Reddy et al. [14], in which they study the effects of delay on a limit cycle in the case of coupled oscillators. In their work, they show that for a set of values for the coupling strength between the oscillators and the delay time, the perturbed limit cycle cannot be induced to oscillate over a threshold. Strogatz names this lack of oscillation "death by delay". From the results seen in Figure 12, the slave neuron shows death by delay for an excitatory synaptic current with maximal conductance $g_A = 10\,nS$.

2.1.4.   Master-Slave-Interneuron

For this motif, in contrast with the master-slave case, the phase response curve was only calculated for a biologically plausible synapse. In this instance, the timing of the excitatory and inhibitory perturbations can be distinct, which will result in a different synaptic current. Three situations were studied: first, when both excitatory and inhibitory neurotransmitter receptors are activated at the same time; second, when the excitatory receptors are activated before the inhibitory, and last, when the inhibitory receptors are activated before the excitatory. As in the previous master-slave motif, the phase response curve was computed for the three different cases. The results are shown in Figure 13. In this image, it can be seen that the PRC is greatly dependant on the timing of the stimulus, as none of the cases are alike. Represented in green in Figure 13a, the neuron was perturbed with both stimuli arriving at the same time; comparing the PRC with that obtained for an inhibitory synapse, it can be seen that they have the same behaviour, from which can

be deduced that the inhibitory synapse has a greater importance, due to the paramaters used in this case, as the maximal conductance for the inhibitory synapse is greater, as is the fraction of bound neurotransmitters, whereas the equilibrium potential contributes to making the inhibitory synaptic current more negative, in contrast to the excitatory synapse. Depicted in pink in Figure 13b, the inhibitory stimulus arrived at the neuron before the excitatory did. As a result, the shape of the PRC enhances the inhibitory behaviour. Finally, shown in orange in Figure 13c, the excitatory current perturbs the neuron before the inhibitory does, hence completely changing the behaviour of the phase response curve, showing a PRC of the same shape as those for an excitatory input as seen both in the cases of rectangular pulses and the excitatory biologically plausible synapse.

3.   Discussion

Throughout this work, the phase response curves for different current inputs were studied, for two neuronal circuits: the master-slave motif, and the master-slave-interneuron. The relevance of analysing the PRCs for different inputs is that it is an experimentally assessable tool that explains the synchronization of dynamical systems.

Firstly, the master-slave neuron motif was studied. In this case, the phase response curves for both rectangular currents, that are theoretical, and biologically plausible synaptic currents were computed. The prediction from the theoretical rectangular currents is that, for excitatory (positive) perturbations that occur close to the previous, unperturbed spike of the membrane potential, the next spike will be delayed, and as the timing of the perturbation advances, the next spike becomes advanced. This result was inverse for the inhibitory (negative) perturbations, although it was not a reflection of the excitatory perturbation. For a biologically plausible current, only the excitatory case was evaluated, showing the same behaviour as the theoretical prediction. However, for a maximal conductance of $g_A = 10\,nS$, the membrane potential showed death by delay for a range of times of perturbation.

The master-slave-interneuron was later analysed. The phase response curves exhibit both excitatory or inhibitory behaviours, depending on the timing of the perturbation. The radical changes observed in the PRCs confirm that the shape of the phase response curve depends on the shape of the stimulus, as well as their timing.

These are, however, preliminary results that are in need of further discussion, as understanding the dynamics of biologically plausible neuronal systems is not an easy task. Additional studies, such as the calculation of the phase response curves for the master-slave-interneuron circuit with rectangular current inputs would add more information about the theoretical predicion of the behaviour of the motif.

Additionally, the same study could be carried out for a model that exhibits type I phase

response curve, that is, it has type I membrane excitability. As the mechanisms through which both types of excitabilities achieve spiking is quite different, the perturbation of the limit cycle in a type I neuron would show a different behaviour.

4. Bibliography

[1] Izhikevich, E. (2007). *Dynamical systems in neuroscience: the geometry of excitability and bursting*. Cambridge, Massachusetts: The MIT Press.

[2] Dayan, P. and Abbott, L.F. (2001). *Theoretical neuroscience: computational and mathematical modeling of neural systems*. Cambridge, Massachusetts: The MIT Press.

[3] Hodgkin, A.L. and Huxley, A.F. (1952). A quantitative description of membrane current and its application to conduction and excitation in nerve. *J. Neurophysiol., 117*, 500-544.

[4] Sterratt, D., Graham, B., Gillies, A. and Willshaw, D. (2011). *Principles of computational modelling in neuroscience*. Cambridge, United Kingdom: Cambride University Press.

[5] Morris, C. and Lecar, H. (1981). Voltage oscillations in the barnacle giant muscle fiber. *Biophys. J., 35*, 193-213.

[6] Izhikevich, E. M. (2004). Which model to use for cortical spiking neurons? *IEEE Transactions on neural networks, 15(5)*, 1063.

[7] Izhikevich, E. M. (2003). Simple model of spiking neurons. *IEEE Transactions on neural networks, 14(6)*, 1569.

[8] Hodgkin, A. L. (1948). The local electric changes associated with repetitive action in a non-medullated axon. *J. Physiol., 107*, 165-181.

[9] Matias, F. S. (2014). *Anticipated synchronization in neuronal circuits*. PhD, Universidade Federal de Pernambuco, Universitat de les Illes Balears. (Access at http://hdl.handle.net/10803/145929).

[10] Canavier, C. (2006). Phase response curve. *Scholarpedia, 1(12)*, 1332.

[11] Smeal, R. M., Ermentrout, B. and G. B., White, J. A. (2010). Phase response curves and synchronized neural networks. *Phil. Trans. R. Soc. B., 365*, 2407-2422.

[12] Ermentrout, B. (1996). Type I membranes, phase resetting curves, and synchrony. *Neural computation, 8*, 979-1001.

[13] Strogatz, S. H. (1998). Death by delay. *Nature, 394*, 316-317.

[14] Ramana Reddy, D. V., Sen, A. and Johnston, G. L. (1998). Time delay induced death in coupled limit cycle oscillators. *Phys. Rev. Lett., 80(23)*, 5109-5112.